2. Details on ligation are based mostly on an analysis of the *parallel* component of the ^{63}Cu hyperfine tensor, because of the higher resolution possible in multifrequency ESR spectra.

3. After one cycle of drying the membranes and soaking with acetonitrile two ^{14}N ligands around Cu^{2+} are deduced for CH_3CN and *none* for CD_3CN. The isotope effect is due to the difference in the solvation energies of the sulfonic groups and cations with deuteriated and protiated solvents.

4. The components of the superhyperfine tensor from ^{14}N have been deduced, taking into consideration the *apparent* tensor values determined along the parallel and perpendicular directions of the **g** tensor.

5. Ligation details are deduced from multifrequency ESR: spectra at X-band are very important for deducing the **g**-tensor components; spectra at C-band are critical for the determining the ratio of the distribution parameters due to strain, $\delta g/\delta A$; the enhanced resolution for the signals corresponding to $m_I = -3/2$ and $-1/2$ at C-band, to $m_I = -3/2$ at X-band, and to $m_I = -1/2$ at S-band is crucial for determining the many parameters involved in the simulation of experimental results.

Acknowledgment. This research was supported by the National Science Foundation Grant DMR-8718947 (ROW). The X-band spectrometer was purchased with NSF equipment Grant DMR-8501312. Experiments at C-, S-, and L-bands were supported by NIH Grant RR-01008 to the National Biomedical ESR Center in Milwaukee, WI. We thank Christopher C. Felix and William E. Antholine for their assistance and for sharing with us their expertise in multifrequency ESR techniques. We also thank the referees for their helpful and constructive comments.

Selective Two-Dimensional NMR Experiments for Topological Filtration of Fragments of Coupling Networks

Lyndon Emsley and Geoffrey Bodenhausen*

Contribution from the Section de Chimie, Université de Lausanne, Rue de la Barre 2, CH 1005 Lausanne, Switzerland. *Received October 31, 1990*

Abstract: In high-resolution NMR, a network of scalar-coupled spins can be broken down into fragments which encode information about the chemical shifts and couplings that are relevant to a cross-peak multiplet in a two-dimensional correlation ("COSY") experiment. Novel selective two-dimensional NMR correlation methods ("soft-COSY") are described which allow one to identify fragments on the basis of their topology. These new experiments allow one to "zoom in" on complicated cross-peak multiplets and include "passive spin filters" (PSFs), consisting of selective inversion pulses applied at the frequencies of passive coupling partners, i.e. spins that are not directly observed in the cross-peak multiplets under investigation. It is demonstrated how such PSFs can be inserted at various points in two-dimensional experiments and how such experiments can be characterized in terms of topology. The topology, couplings, and shifts of a fragment may be represented by a matrix **M**, while a selective experiment can be represented by a matrix **P**. Several degrees of matching of **M** and **P** can be distinguished. The techniques, which provide a novel method of discriminating and assigning spin systems, are demonstrated on a cyclopropane derivative and the cyclic undecapeptide cyclosporin.

Introduction

Two- and three-dimensional NMR experiments provide convenient methods for determining the parameters of a nuclear spin system, such as chemical shifts and scalar couplings among the protons and other nuclei in molecules dissolved in isotropic solution.[1,2] Traditionally, physical chemists tend to think of couplings and shifts as parameters of the "static" spin Hamiltonian (averaged over molecular motion), while organic chemists often prefer an interpretation which emphasizes the role of the chemical environment (substituent effects, etc.). With the development of multidimensional spectroscopy, a third formulation is beginning to emerge, which may help to bridge the gap. This description depicts the ensemble of spins and their mutual couplings by a *coupling network*. In such a graph, the spins (for example protons) are represented by *nodes* and the couplings by *edges*. A coupling network is a chromatic graph, since the nodes carry information about the chemical shifts (which might be represented by a frequency or "color", e.g. a shift expressed in ppm with respect to a standard) while the edges are labeled by the magnitude and sign of the couplings (also in units of frequency, usually in Hz). Strickly speaking, such a graph is nothing but a representation of the Hamiltonian and contains neither more nor less information than a table of shifts and couplings. The great advantage of a graph however lies in that it can be easily partitioned into subgraphs which we call *fragments*. A network with n scalar couplings can be split into n fragments. A fragment can be defined so as to contain all the information that is relevant to the frequency coordinates and fine structure of a cross-peak multiplet in a two-dimensional spectrum. Such a fragment F^{kl} consists of two active nodes A^k and A^l, plus all passive nodes P_i^{kl} coupled to the active nodes. We must distinguish *cyclic* passive nodes that are connected to both active nodes and *noncyclic* passive nodes which are coupled only to one active node. In earlier studies,[3,4] only the chemical shifts of the active nodes were considered relevant to the definition of a fragment, while in this paper the shifts of the passive nodes are also essential. On the other hand, while in earlier studies we had to consider the actual magnitudes of the couplings (and, in the case of cyclic passive nodes, also their relative signs) we are now primarily interested in the "topological" question of whether a coupling is observable or can be neglected.

There is a wide range of two-dimensional NMR experiments that may help to determine the parameters of a coupling network. Correlation spectroscopy ("COSY") and its many relatives, including variants such as multiple-quantum NMR, can be used for this purpose.[1,2,5-10] By and large, however, all of these

(1) Sanders, J. K. M.; Hunter, B. K. *Modern NMR Spectroscopy: A Guide for Chemists*; Oxford University Press: Oxford, 1987.
(2) Ernst, R. R.; Bodenhausen, G.; Wokaun, A. *Principles of Nuclear Magnetic Resonance in One and Two Dimensions*; Clarendon: Oxford, 1987.
(3) Pfändler, P.; Bodenhausen, G. *J. Magn. Reson.* **1988**, *79*, 99.
(4) Pfändler, P.; Bodenhausen, G. *J. Magn. Reson.* **1990**, *87*, 26.
(5) Jeener, J. *Ampère International Summer* School; Basko Polje, Yugoslavia, 1971.
(6) Aue, W. P.; Bartholdi, E.; Ernst, R. R. *J. Chem. Phys.* **1976**, *64*, 2229.

0002-7863/91/1513-3309$02.50/0

techniques have their limitations: the assignment of multiplets to fragments is often ambiguous, either for fundamental reasons (since several distinct fragments may be mapped into indistinguishable multiplets) or, more commonly, because of poor digital resolution, overlap, strong coupling, or any combination of these.[11] Problematic assignments can usually be identified as such, either by simple inspection of the experimental multiplet or in the course of computer-supported analysis, where any attempt to assemble incompatible fragments should be signalled by poor likelihood factors.[4] Many ambiguities in the assignment of multiplets to fragments may be overcome simply by increasing the digital resolution, i.e. by "zooming in" on problematic multiplets. This can easily be achieved by selective ("soft") COSY,[12-15] which can yield a spectrum of a chosen multiplet with a very high resolution, since the spectral width is quite narrow (typically 20 to 60 Hz in the ω_1 dimension) and the digital resolution can therefore be quite high (say 10 points per Hz). Nevertheless ambiguities remain even if the resolution can be enhanced at will.

In recent years, Levitt and Ernst[16] and Radloff and Ernst[17] have proposed sophisticated pulse schemes that are tailored to elicit responses from coupling networks with a chosen topology. Some of these schemes rely on the spin-topology-selective excitation of multiple-quantum coherences of the highest possible order (so-called total spin coherence filters or T-filters). Alternatively, one may use pulse sequences where the time segmentation is varied randomly in order to remove signals from undesirable networks (so-called averaged evolution filters or A-filters). While these methods represent milestones in the development of multidimensional spectroscopy, their practical applications are limited by the requirement that all couplings should have a reasonably uniform magnitude. Thus Radloff and Ernst write[17] "we allow, clearly as an oversimplification of the actual situation, for only one numerical value J of all coupling constants that do not vanish". This implies that coupling networks must be represented by nonchromatic "black-and-white" graphs, whereas actual systems do not easily fit into this Procrustean bed. Furthermore, these filtration techniques are not fragment-oriented and may run into problems when applied to networks that are more extensive (e.g. complex alcohols or esters currently of interest to Radloff[18]) than the elementary topologies for which they are designed.

Freeman and co-workers have developed alternative strategies, dubbed DAISY (*d*irect *a*ssignment *i*nterconnection *s*pectroscopy), using sequences of selective pulses that are applied in succession to different multiplets that are believed to belong to a common coupling network.[19-25] Their so-called *zz*-pulses are semiselective composite radiofrequency pulses that excite longitudinal two-spin order $2I_z^{A1}I_z^{A2}$ between two selected spins I^{A1} and I^{A2}. So-called *zzz*-pulses allow one to convert $2I_z^{A1}I_z^{A2}$ into $2I_z^{A2}I_z^{A3}$, and from there into $2I_z^{A3}I_z^{A4}$, etc. If the populations of the spins at the end of the chain are affected, this confirms that the hypothesis about the existence of such a chain is indeed correct.

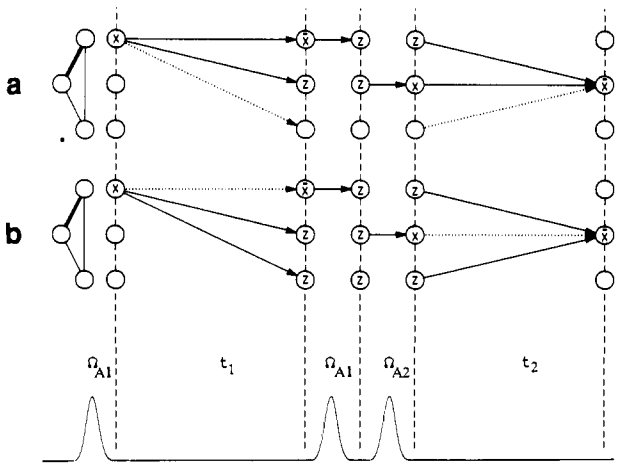

Figure 1. Product operator evolution graphs and pulse sequence suitable for selective correlation experiments: (a) pathway involving two-spin order $2I_z^{A1}I_z^{A2}$ in a three-spin system, and (b) pathway involving three-spin order $4I_z^{A1}I_z^{A2}I_z^{P1}$.

This paper represents an extension and generalization of recent developments in our laboratory.[15,26,27] We shall focus attention on semiselective ("soft") correlation experiments that allow one to record one two-dimensional multiplet at a time. Self-refocusing 270° Gaussian pulses[14] are combined with G^3 Gaussian pulse cascades[28] for selective excitation of active spins and selective inversion of passive spins, respectively. By inverting passive spins selectively, and by making use of difference spectroscopy, the new idea of a "passive spin filter" (PSF) can be realized. Various combinations lead to a class of experiments which we have dubbed selectively inverted soft correlation spectroscopy, SIS-(p,q)-COSY.

Methods

Selective Correlation Spectroscopy. Consider the pulse sequence of Figure 1. At the beginning of the sequence, a semiselective pulse is applied at the chemical shift Ω_{A1} to the multiplet of spin I^{A1} to create in-phase magnetization I_x^{A1} which evolves during t_1 under the effect of the J coupling and chemical shift into antiphase coherence $2I_x^{A1}I_z^{A2}$. Another semiselective pulse applied at the same frequency converts this into longitudinal two-spin order $2I_z^{A1}I_z^{A2}$, which is subsequently converted into antiphase coherence of the other spin $2I_z^{A1}I_x^{A2}$ by a third semiselective pulse applied at the chemical shift Ω_{A2}. This coherence then evolves into observable in-phase coherence I_x^{A2} during t_2.

The semiselective pulses in these experiments should be such that I_z is converted into pure I_x. In practice this means that, over the width of a multiplet (typically 20–50 Hz), the pulse must produce magnetization with a constant phase as a function of offset from the transmitter. This can be achieved with self-refocusing 270° Gaussian shaped pulses.[14] It may sometimes be necessary to use more sophisticated pulses such as G^4 Gaussian pulse cascades[28] or so-called BURP pulses.[29] All three types of pulse give good selectivity with a "top hat" profile in frequency domain, but we tend to prefer 270° Gaussian pulses because they are relatively short (typically 35 ms to excite a multiplet 30 Hz wide) so that relaxation during the pulse can largely be neglected.

The product operator[30] evolution graphs[31] of Figure 1, a and b, show how in a weakly coupled three-spin system the magnetization may follow either of the two pathways shown. For the

(7) Piantini, U.; Sørensen, O. W.; Ernst, R. R. *J. Am. Chem. Soc.* **1982**, *104*, 6800.
(8) Shaka, A. J.; Freeman, R. *J. Magn. Reson.* **1983**, *51*, 169.
(9) Rance, M.; Sørensen, O. W.; Bodenhausen, G.; Wagner, G.; Ernst, R. R.; Wüthrich, K. *Biochem. Biophys. Res. Commun.* **1983**, *117*, 479.
(10) Weitekamp, D. P. *Adv. Magn. Reson.* **1983**, *11*, 111.
(11) Pfändler, P.; Bodenhausen, G. *Magn. Reson. Chem.* **1988**, *26*, 888.
(12) Brüschweiler, R.; Madsen, J. C.; Griesinger, C.; Sørensen, O. W.; Ernst, R. R. *J. Magn. Reson.* **1987**, *73*, 380.
(13) Cavanagh, J.; Waltho, J. P.; Keeler, J. *J. Magn. Reson.* **1987**, *74*, 386.
(14) Emsley, L.; Bodenhausen, G. *J. Magn. Reson.* **1989**, *82*, 211.
(15) Emsley, L.; Bodenhausen, G. *Computational Aspects of the Study of Biological Macromolecules by NMR Spectroscopy. Proceedings of the NATO Advanced Research Workshop*; Il Ciocco, Italy, June 1990, in press.
(16) Levitt, M. H.; Ernst, R. R. *J. Chem. Phys.* **1985**, *83*, 3297.
(17) Radloff, C.; Ernst, R. R. *Mol. Phys.* **1989**, *66*, 161.
(18) Radloff, S.; Radloff, C. *Ars Bibendi*; Hombrechtikon Press: Zurich, 1990.
(19) Friedrich, J.; Davies, S.; Freeman, R. *J. Magn. Reson.* **1987**, *75*, 390.
(20) Davies, S.; Friedrich, J.; Freeman, R. *J. Magn. Reson.* **1987**, *75*, 540.
(21) Freeman, R.; Friedrich, J.; Davies, S. *Magn. Reson. Chem.* **1988**, *26*, 903.
(22) Davies, S.; Friedrich, J.; Freeman, R. *J. Magn. Reson.* **1987**, *75*, 540.
(23) Friedrich, J.; Davies, S.; Freeman, R. *Mol. Phys.* **1988**, *64*, 691.
(24) Friedrich, J.; Davies, S.; Freeman, R. *J. Magn. Reson.* **1988**, *80*, 168.
(25) Xu, P.; Wu, X. L.; Freeman, R. *J. Magn. Reson.* **1990**, *89*, 198.
(26) Emsley, L.; Huber, P.; Bodenhausen, G. *Angew. Chem.* **1990**, *102*, 576; *Angew. Chem., Int. Ed. Engl.* **1990**, *29*, 517.
(27) Müller, N.; Di Bari, L.; Bodenhausen, G. *J. Magn. Reson.* In press.
(28) Emsley, L.; Bodenhausen, G. *Chem. Phys. Lett.* **1990**, *165*, 169.
(29) Geen, H.; Wimperis, S.; Freeman, R. *J. Magn. Reson.* **1989**, *85*, 620.
(30) Sørensen, O. W.; Eich, G. W.; Levitt, M. H.; Bodenhausen, G.; Ernst, R. R. *Prog. NMR Spectrosc.* **1983**, *16*, 163.
(31) Eggenberger, U.; Bodenhausen, G. *Angew. Chem.* **1990**, *102*, 392; *Angew. Chem., Int. Ed. Engl.* **1990**, *29*, 374.

pathway through $2I_z^{A1}I_z^{A2}$, the time-domain modulation of the relevant term in the density operator[2,30] is given by

$$\sigma(t_1,t_2) = -I_x^{A2} \sin(\Omega_{A1}t_1) \sin(\pi J_{A1A2}t_1) \cos(\pi J_{A1P1}t_1) \times \sin(\Omega_{A2}t_2) \sin(\pi J_{A1A2}t_2) \cos(\pi J_{A2P1}t_2) \quad (1)$$

On the other hand, for the pathway through $4I_z^{A1}I_z^{A2}I_z^{P1}$ we obtain a contribution

$$\sigma(t_1,t_2) = -I_x^{A2} \cos(\Omega_{A1}t_1) \sin(\pi J_{A1A2}t_1) \sin(\pi J_{A1P1}t_1) \times \cos(\Omega_{A2}t_2) \sin(\pi J_{A1A2}t_2) \sin(\pi J_{A2P1}t_2) \quad (2)$$

Addition of eqs 1 and 2 followed by some elementary trigonometry gives

$$\sigma(t_1,t_2) = -\tfrac{1}{2}I_x^{A2} \sin(\pi J_{A1A2}t_1) \sin(\pi J_{A1A2}t_2) \times \{\sin((\Omega_{A1} + \pi J_{A1P1})t_1) \sin((\Omega_{A2} + \pi J_{A2P1})t_2) + \sin((\Omega_{A1} - \pi J_{A1P1})t_1) \sin((\Omega_{A2} - \pi J_{A2P1})t_2)\} \quad (3)$$

which corresponds to the experimentally observed signal.[32] More specifically, the $\sin((\Omega_{Ai} \pm \pi J_{Ai/P1})t_i)$ terms correspond to apparent shifts of the two subspectra and the $\sin(\pi J_{A1A2}t_i)$ terms correspond to an antiphase splitting. Thus the pattern is an antiphase square repeated twice and displaced by a vector $\mathbf{J}_{P1} = (J_{A1P1}, J_{A2P1})$. Note that it is the freedom to follow either of the two pathways of Figure 1, a or b (involving either two- or three-spin order), that results in the characteristic multiplet structure for a three-spin system. In fragments containing n passive spins, one observes a super- or juxtaposition of 2^n antiphase squares, each consisting of two positive and two negative peaks, separated by displacement vectors $\mathbf{J}_{Pi} = (J_{A1Pi}, J_{A2Pi})$ for $i = 1...n$. The fine structure of the multiplets obtained in this manner obeys the same rules as in conventional COSY with a small flip angle,[6] z-filtered COSY,[33,34] in E.COSY,[35,36] or in PE.COSY.[37]

Such multiplets are very informative, particularly if the digital resolution is high, as can easily be achieved with soft-COSY without running into excessively time-consuming experiments.[13,15] Yet such spectra can remain unintelligible if there are extensive overlaps, and it is therefore highly desirable to find some means to separate overlapping multiplets. Even in the absence of overlaps, the complexity of the interplay of the displacement vectors, or uncertainties regarding which passive spin causes which displacement, can be so daunting that recourse to special techniques may be necessary to assist interpretation.

Passive Spin Filters. Of the two contributions of eqs 1 and 2, the former could occur in any system with a resolved coupling J_{A1A2}, while the latter only has a nonvanishing amplitude if both J_{A1P1} and J_{A2P1} are non-zero. It is possible to discriminate between these two pathways with a *passive spin filter* (PSF) which involves the selective manipulation of I^{P1}. This can be realized by applying a $\pi/2$ pulse to the passive spin during the mixing time τ_m between the last two pulses of the experiment to bring about the transformation

$$4I_z^{A1}I_z^{A2}I_z^{P1} \xrightarrow{1/2\pi I_y^{P1}} 4I_z^{A1}I_z^{A2}I_x^{P1} \quad (4)$$

and then reverse this process by another selective $\pi/2$ pulse. Phase cycling allows one to discard signal contributions that do not involve this two-step process. If we observe a cross-peak between the two *active* species with this scheme, this is evidence that they are both connected to the *passive* spin which was manipulated during τ_m, i.e. that the three spins form a fragment with a cyclic coupling topology.

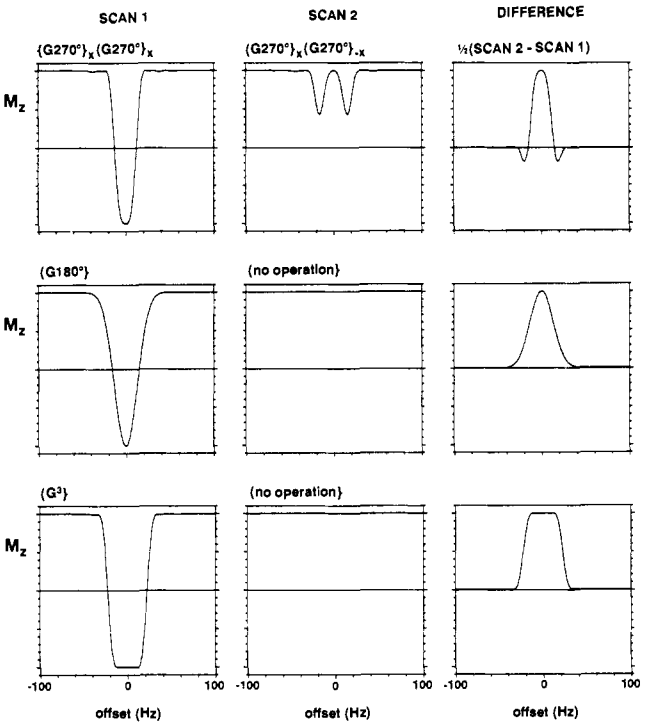

Figure 2. Response as a function of offset of the longitudinal magnetization I_z to passive spin filters consisting (top) of two 270° Gaussian pulses with phase-alternation in the manner of eq 5, (middle) with the "on/off" scheme, i.e., with a 180° Gaussian inversion pulse on odd transients only, and (bottom) with a G^3 pulse cascade for selective inversion on odd transients only. The plots in the right-hand column represent the frequency selectivity of each PSF.

A passive spin filter designed to retain terms that involve spin I^{Pi} could be implemented by *phase-alternating* semiselective self-refocusing Gaussian pulses[14] applied at Ω_{Pi}:

$$\begin{array}{lll} (3\pi/2)(3\pi/2) & \text{add} & \\ (3\pi/2)(-3\pi/2) & \text{subtract} & (5) \end{array}$$

On closer inspection, however, we may simplify this sequence even further. The first step corresponds to a semiselective 180° inversion pulse applied to I^{Pi}, while the second step should ideally leave the system unperturbed. Thus a PSF can most simply be implemented by applying a soft 180° inversion pulse on alternate scans, preferably using a G^3 Gaussian pulse cascade.[28] In a similar vein hard 180° pulses have been applied to heteronuclei on alternate scans to achieve filtering of protons attached to ^{13}C or ^{15}N, for example, in nonselective COSY or NOESY experiments.[38] For nonselective experiments there is no particular advantage in using either of the above schemes, and indeed both have been used.[38] However, when using shaped selective pulses we see that the "on/off" scheme actually leads to *better frequency selectivity* than phase alternation, as illustrated in Figure 2. We therefore use the on/off scheme rather than phase alternation for selective passive-spin filtration. One should also take into account the durations of the pulses. For the comparison of Figure 2, the pulse widths are the same, so as to obtain approximately the same bandwidth, i.e. we compare two 50 ms 270° Gaussian pulses in Figure 2a with one 100 ms G^3 pulse in Figure 2c. The bandwidth of the filter is about 40 Hz in each case. Better frequency selectivity could be achieved in the phase-alternated version by using more sophisticated pulses instead of 270° Gaussians, such as G^4 Gaussian pulse cascades,[28] but such pulse sequences tend to be relatively long, and relaxation during the pulses might lead to signal losses. In general, the shorter the pulses are, the broader

(32) (a) One may be tempted to conclude that the pathway of eq 1 always has zero intensity since $\sin(\Omega_{A1}t_1)$ is zero on resonance. However, the standard practice of incrementing the phase of the first pulse from one t_1 increment to another (time proportional phase incrementation, or TPPI)[2,32b] ensures that this is not the case. (b) Drobny, G.; Pines, A.; Sinton, S.; Weitekamp, D.; Wemmer, D. *Faraday Div. Chem. Soc. Symp.* **1979**, *13*, 49.

(33) Oschkinat, H.; Pastore, A.; Pfändler, P.; Bodenhausen, G. *J. Magn. Reson.* **1986**, *69*, 559.

(34) Pfändler, P.; Bodenhausen, G. *J. Magn. Reson.* **1987**, *72*, 475.

(35) Griesinger, C.; Sørensen, O. W.; Ernst, R. R. *J. Am. Chem. Soc.* **1985**, *107*, 6394.

(36) Griesinger, C.; Sørensen, O. W.; Ernst, R. R. *J. Chem. Phys.* **1986**, *85*, 6837.

(37) Müller, L. *J. Magn. Reson.* **1987**, *72*, 91.

(38) Otting, G. *Q. Rev. Biophys.* **1990**, *23*, 39.

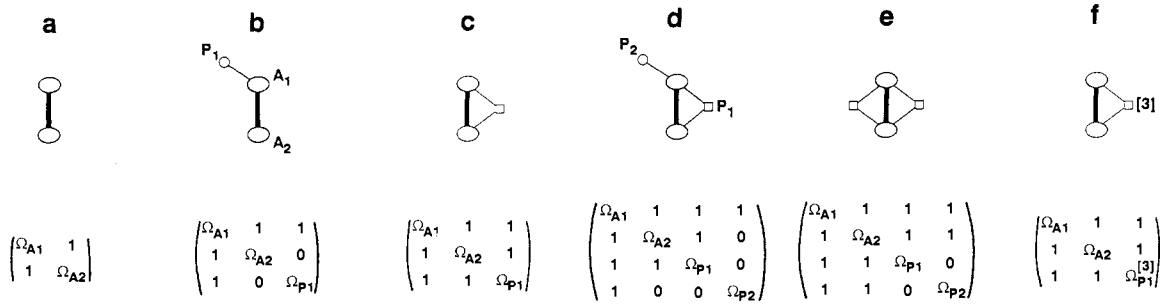

Figure 3. Graphical representations of some typical fragments of coupling networks and corresponding **M** matrices. Heavy lines connect the active spins I^{A1} and I^{A2} while lighter lines indicate couplings to passive spins. Diagonal elements in **M** represent the chemical shifts, and the off-diagonal elements indicate the presence or absence of resolved couplings (see text). The symbol [3] in the last example indicates that there are three equivalent passive spins, as in a methyl group.

the bandwidth of the filter, so that in applications to large molecules with short T_2's (less than, say, 100 ms) one might be forced to sacrifice some frequency selectivity in order to reduce sensitivity losses due to relaxation. In most applications, however, passive spin filters which affect only one multiplet (requiring one or two pulses of total duration 100 ms) do not give rise to significant sensitivity losses.

Fragments of Coupling Networks. In our terminology, a coupling network[3,4] is fully characterized by its topology, the chemical shifts of the nodes, and the scalar coupling constants (including their signs) associated with the edges. We shall begin by segmenting the global network into fragments as defined in the introduction. We may represent a fragment of n spins by a symmetric $n \times n$ matrix **M** with diagonal elements M_{ii} corresponding to the chemical shifts Ω_i of the n sites and off-diagonal elements M_{ij} corresponding to scalar couplings between spins i and j. Since we shall discuss experiments which only depend on the presence or absence of couplings, we may define the elements M_{ij} to be either 1 (if the coupling is sufficient to give rise to a cross-peak multiplet) or 0 (if the coupling is too weak to be detected, i.e. if J is much smaller than the effective line width). The border depends on the effective resolution of the experiment. For example, a noncyclic three-spin fragment with $J_{AX} = 0$ is described by a matrix

$$\mathbf{M} = \begin{bmatrix} \Omega_A & 1 & 0 \\ 1 & \Omega_M & 1 \\ 0 & 1 & \Omega_X \end{bmatrix} \tag{6}$$

regardless of the actual values of J_{AM} and J_{MX}, provided only that both couplings are resolved. Although the diagonal elements of the matrix **M** contain "chromatic" information about the shifts, the off-diagonal elements of the matrix **M** represent purely topological information. (We should note in passing that in the context of other experiments, it might be useful to opt for a fully chromatic matrix representation, where the off-diagonal elements would indicate the magnitudes and signs of the couplings.) In the present paper, we shall always adhere to the convention that the element M_{11} gives the chemical shift of the spin I^{A1} which is active during the evolution interval t_1 and the element M_{22} the shift of the spin I^{A2} which is active in the detection period t_2. Elements M_{ii} ($3 \le i \le n$) correspond to passive spins P_i in order of increasing chemical shift. It is also possible to use graphical representations of fragments as shown in the upper part of Figure 3, which are essentially equivalent to the matrix representations shown in the lower part of the figure.[3]

Probing Fragment Topologies. Our experiments are designed to discriminate and assign fragments based on the structure of the matrix **M** or of submatrices thereof. We define a matrix **P** for each experiment which has a similar structure to **M** but may have different dimensions. For a simple soft-COSY experiment to yield a cross-peak multiplet, the RF carrier frequencies must be in the vicinity of Ω_{A1} and Ω_{A2}, and there must be a resolved coupling J_{A1A2} between the two active spins I^{A1} and I^{A2} for coherence transfer to occur (otherwise the terms $\sin(\pi J_{A1A2}t_1)$ and $\sin(\pi J_{A1A2}t_2)$ in eqs 1–3 would vanish). The corresponding **P** matrix is defined to be

$$\mathbf{P} = \begin{bmatrix} \Omega_{A1} & 1 \\ 1 & \Omega_{A2} \end{bmatrix} \tag{7}$$

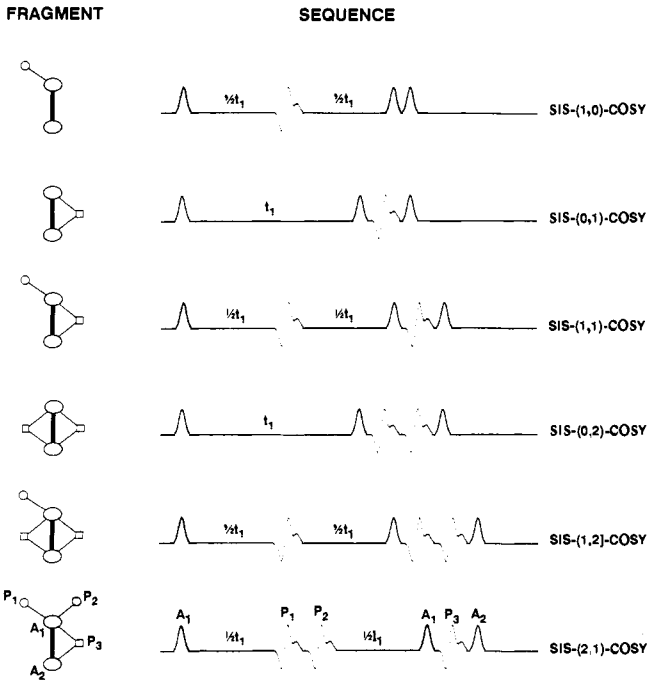

Figure 4. Pulse sequences suitable for various SIS-(p,q)-COSY experiments, together with graphical representations of their associated topologies. A solid pulse should be applied on every scan, while a dotted pulse is applied only on alternate scans (see text).

Thus we can confer topological properties which are characterized by the **P** matrix to a given NMR experiment. The **P** matrix of eq 7 for the soft-COSY experiment corresponds to the same topology as the fragment shown in Figure 3a. In order to demonstrate the logic behind the construction of the **P** matrices we give several examples below.

Inclusion of one PSF at Ω_{P1} in the mixing period of soft-COSY implies that three-spin order $4I_z^{A1}I_z^{A2}I_z^{P1}$ must be present in this interval. Only if the passive spin is coupled to *both* active spins can this experiment produce a multiplet. Thus the matrix representation of such an experiment is

$$\mathbf{P} = \begin{bmatrix} \Omega_{A1} & 1 & 1 \\ 1 & \Omega_{A2} & 1 \\ 1 & 1 & \Omega_{P1} \end{bmatrix} \tag{8}$$

We shall use the name SIS-(0,1)-COSY for this experiment (see Figure 4). In general the experiments are called SIS-(p,q)-COSY where p refers to the number of PSFs in the evolution period (see

below) and q refers to the number of PSFs in the mixing period. Since longitudinal three-spin order must be involved in SIS-(0,1)-COSY, coherence transfer is *restricted to only the pathway* shown in the lower part of Figure 1, and the signals are modulated according to eq 2. In the case of a three-spin system the result is a multiplet structure which is doubly antiphase with respect to J_{A1A2} and J_{A1P1} in ω_1 and with respect to J_{A1A2} and J_{A2P1} in ω_2. This yields the same multiplet structure as triple-quantum-filtered COSY.[39] Indeed, although we never create triple-quantum coherence, the conditions for the existence of the cross-peak multiplet are the same. We are probing the ability of the system to sustain a particular operator product, in this case $4I_z^{A1}I_z^{A2}I_z^{P1}$. In contrast to triple-quantum-filtered COSY, any additional couplings to further spins I^{Pi} will give rise to a characteristic juxtaposition of two of these basic doubly antiphase patterns separated by a vector corresponding to the passive splitting J_{A1Pi} in ω_1 and J_{A2Pi} in ω_2.

Thus it can be seen that a nonvanishing off-diagonal element P_{ij} represents the requirement for a resolved coupling between spins i and j for the experiment to work. Furthermore, we see that by including an arbitrary number of PSFs in a soft-COSY experiment we can engineer probes that are associated with almost any topology. Inclusion of two PSFs at Ω_{P1} and Ω_{P2} in the mixing period requires that four-spin order $8I_z^{A1}I_z^{A2}I_z^{P1}I_z^{P2}$ must be present. Only if *both* passive spins are coupled to *both* active spins can this experiment produce a multiplet. Thus the matrix **P** is

$$\mathbf{P} = \begin{bmatrix} \Omega_{A1} & 1 & 1 & 1 \\ 1 & \Omega_{A2} & 1 & 1 \\ 1 & 1 & \Omega_{P1} & 0 \\ 1 & 1 & 0 & \Omega_{P2} \end{bmatrix} \quad (9)$$

We shall use the name SIS-(0,2)-COSY for this experiment (see Figure 4). In this case, the multiplet structure observed is similar to quadruple-quantum-filtered COSY,[39] i.e. with a triply antiphase structure in both dimensions.

Selective passive spin filters may also be designed to probe *noncyclic* spin topologies. Instead of placing the PSF in the mixing interval (a τ_m-PSF), we must place it in the center of the evolution period (a t_1-PSF). Thus, during the first half of t_1 the magnetization of spin I^{A1} evolves into antiphase coherence $2I_x^{A1}I_z^{P1}$ or $2I_y^{A1}I_z^{P1}$ with respect to I^{P1}, at which point we apply a PSF to I^{P1}. During the second part of the evolution period the term continues to evolve so that it is no longer in antiphase with respect to I^{P1}. Simultaneously with this process, and throughout t_1, the coherence evolves into $2I_x^{A1}I_z^{A2}$, i.e. in antiphase with respect to the second active spin I^{A2}. Thus, the requirement for this experiment to work is simply that I^{P1} must be connected to I^{A1}, but not necessarily to I^{A2}. Therefore the topological characteristics of an experiment containing a single t_1-PSF are given by

$$\mathbf{P} = \begin{bmatrix} \Omega_{A1} & 1 & 1 \\ 1 & \Omega_{A2} & 0 \\ 1 & 0 & \Omega_{P1} \end{bmatrix} \quad (10)$$

We shall refer to this experiment as SIS-(1,0)-COSY (see Figure 4). Note that the matrix of eq 10 is sparser than that of SIS-(0,1)-COSY in eq 8. Thus the requirement for passage through a SIS-(1,0)-COSY is less stringent than for SIS-(0,1)-COSY.

Similarly, for SIS-(2,0)-COSY we obtain a topology

$$\mathbf{P} = \begin{bmatrix} \Omega_{A1} & 1 & 1 & 1 \\ 1 & \Omega_{A2} & 0 & 0 \\ 1 & 0 & \Omega_{P1} & 0 \\ 1 & 0 & 0 & \Omega_{P2} \end{bmatrix} \quad (11)$$

In general for a SIS-(p,0)-COSY we check whether the system can independently sustain operator products $2^pI_y^{A1}I_z^{P1}...I_z^{Pp}$ and

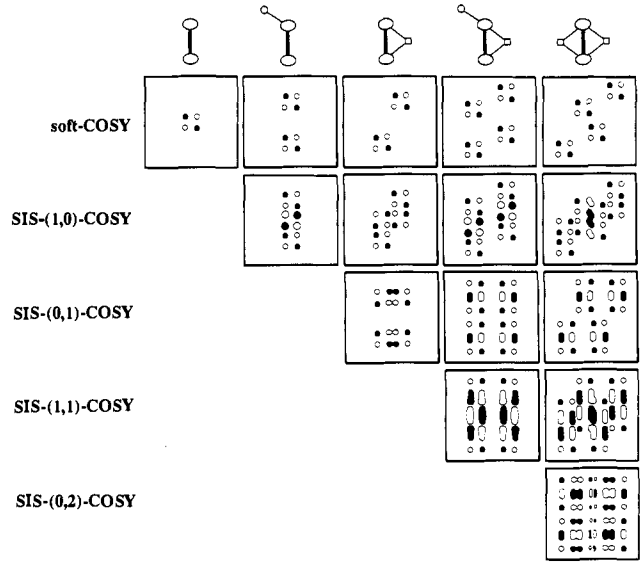

Figure 5. Simulated multiplet patterns expected from the SIS-(p,q)-COSY experiments shown on the left when applied to the fragments shown along the top of the figure. Notice how the structure of the patterns reveals the presence of additional couplings if **M** has more nonvanishing off-diagonal elements than **P**, or if **M** has a higher dimension than **P**. Cases of exact matching (**P** = **M**) are shown along the "diagonal" of the figure. Situations that would belong in the lower left triangle yield no response. Positive peaks have been filled in for clarity.

$2I_z^{A1}I_z^{A2}$, rather than requiring a single product of $q + 2$ operators as in SIS-(0,q)-COSY. As a final example the experiment at the bottom of Figure 4 contains three PSF's, two of which are applied at the frequencies Ω_{P1} and Ω_{P2} in the middle of the evolution interval t_1, while the third is applied at Ω_{P3} during the mixing time. The matrix representing this experiment is

$$\mathbf{P} = \begin{bmatrix} \Omega_{A1} & 1 & 1 & 1 & 1 \\ 1 & \Omega_{A2} & 0 & 0 & 1 \\ 1 & 0 & \Omega_{P1} & 0 & 0 \\ 1 & 0 & 0 & \Omega_{P2} & 0 \\ 1 & 1 & 0 & 0 & \Omega_{P3} \end{bmatrix} \quad (12)$$

This is a SIS-(2,1)-COSY experiment. To sum up, with reference to Figure 4, it can be seen that t_1-PSFs have linear topological character, while τ_m-PSFs are appropriate for cyclic topologies. In Figure 5 we show expected multiplet structures, some of which deserve further comment.

Multiplet Structures in SIS-(p,0)-COSY. The peak structures in these experiments are different from those in all other forms of COSY. For the experiment with $p = 1$ applied to a noncyclic three-spin system, the relevant part of the density operator is modulated by

$$\sigma(t_1,t_2) = -I_x^{A2} \sin(\Omega_{A1}t_1)(\sin(\pi J_{A1P1}{}^1\!/_2 t_1))^2 \times \sin(\pi J_{A1A2}t_1) \sin(\Omega_{A2}t_2) \sin(\pi J_{A1A2}t_2) \quad (13)$$

In the ω_2 dimension this gives rise to an antiphase doublet split by J_{A1A2} and in the ω_1 domain to an antiphase triplet splitting of ${}^1\!/_2 J_{A1P1}$ with intensity ratios −1:2:−1, convoluted with an antiphase J_{A1A2} doublet. This results from the nature of the PSF which *interrupts the evolution of only one coupling* (J_{A1P1}), causing it to be modulated in proportion to ${}^1\!/_2 t_1$, *while it does not interrupt any of the other interactions*, so that all remaining shifts and couplings are modulated in proportion to the whole of t_1. An additional passive spin I^{P2} will give rise to a duplication of two such patterns separated by a displacement vector corresponding to the passive couplings $J(\omega_1,\omega_2) = (J_{A1P2}, J_{A2P2})$. On the other hand, if the spin I^{P1} which is probed by the PSF in the middle of t_1 also has a resolved coupling to the other active spin I^{A2}, i.e., if the coupling fragment is cyclic rather than linear, the multiplet will no longer feature any triplets but will consist of four juxtaposed square patterns having a splitting J_{A1A2}, where the patterns are

(39) Müller, N.; Ernst, R. R.; Wüthrich, K. *J. Am. Chem. Soc.* **1986**, *108*, 6482.

Table I. Possible Outcomes for a Comparison between M^{sub}_{ij} and P_{ij}

case	M_{ij}	P_{ij}	outcome
1	0	0	match
2	1	1	match
3	1	0	pass
4	0	1	fail

each in antiphase with respect to the displacement vectors of $J(\omega_1,\omega_2) = (^1/_2J_{A1P1},0)$ and $(^1/_2J_{A1P1},J_{A2P1})$, as is exemplified in Figure 5. This structure can easily be rationalized by considering the difference between a normal soft-COSY and a modified spectrum in which the J_{A1P1} coupling is refocused in t_1 through selective inversion of the passive spin I^{P1}.

Match or Mismatch? Discrimination between different fragments is achieved on the basis of the degree of matching between the experimental topology **P** and the fragment **M**. The spin system can give several different answers to our specific "question". For perfect matching all elements P_{ij} must equal M_{ij} (**P** = **M**), and in this case the experiment will yield a two-dimensional multiplet with a characteristic pattern (as described above). If dim(**M**) < dim(**P**), i.e. if there are elements in **P** which are not contained in **M**, this corresponds to a case of mismatch, and no multiplet will be observed. In the case where dim(**M**) > dim(**P**), one has to identify a submatrix $\mathbf{M}^{sub}$ by comparing each of the diagonal elements M_{ii} in turn with elements P_{ii}. If $M_{ii} \neq P_{ii}$ then the ith row and column of **M** must be removed. This process is repeated until $M_{ii} = P_{ii}$; the resulting matrix is then the correct submatrix $\mathbf{M}^{sub}$ for comparison with **P**.

If dim($\mathbf{M}^{sub}$) < dim(**P**), this corresponds to a case of mismatch, and no multiplet will be observed. If dim($\mathbf{M}^{sub}$) = dim(**P**), we compare their off-diagonal elements. Notice that, according to the above recipe for constructing $\mathbf{M}^{sub}$, dim($\mathbf{M}^{sub}$) cannot be larger than dim(**P**). Note also that elements connecting passive spins are defined to be 0 in **P**, although our experiments do not probe couplings between passive spins and therefore cannot give any information about topological properties associated with such couplings. As a result we only have to compare off-diagonal elements of **P** and **M** in the first two rows. If we compare an element M_{ij}^{sub} with the corresponding P_{ij} there are four possible outcomes, listed in Table I. Either of the first two outcomes corresponds to a perfect match. The third outcome, although not a perfect match, is distinguishable from our spectra (see below). The fourth outcome in Table I is a definite mismatch, since our test requires a coupling which does not exist in the actual fragment.

To sum up, having compared all appropriate elements M_{ij}^{sub} with P_{ij}, we can distinguish three degrees of matching between **P** and **M**: (i) **P** = **M**; (ii) **P** = $\mathbf{M}^{sub}$; (iii) **P** matches **M** or $\mathbf{M}^{sub}$, but there is at least one more coupling in **M** than in **P** (at least one occurrence of condition 3 in Table I). We can distinguish two levels of mismatch between **P** and **M**, both leading to a vanishing response: (iv) dim(**M**) < dim(**P**) or dim($\mathbf{M}^{sub}$) < dim(**P**) and (v) **P** matches the dimension of **M** or $\mathbf{M}^{sub}$, but there is at least one coupling more in **P** than in **M** (at least one occurrence of condition 4 in Table I). As we will see below, cases i, ii, and iii produce similar but easily distinguishable results, while cases iv and v cannot be distinguished experimentally.

To avoid mismatch in an SIS-(0,q)-COSY the tested fragment must fulfill the condition that

$$\sum M^{sub}_{1j}M^{sub}_{2j}P_{1j}P_{2j} = q \qquad (14)$$

where the summation must extend over all columns j except the first two (j = 3...n). If eq 14 is not satisfied the resulting multiplet will have zero intensity. For SIS-(p,0)-COSY, however, one obtains in analogy to eq 14 a simple expression

$$\sum M^{sub}_{1j}P_{1j} = p \qquad (15)$$

where the summation must extend over all columns except the first two (j = 3...n).

For the condition of perfect matching we can simply express the criteria in terms of the graphical representations of the matrices, so that a spin system **M** and a sequence **P** match if **P** can be superimposed on **M** such that for every edge and node of **P** there exists an edge and node in **M**.

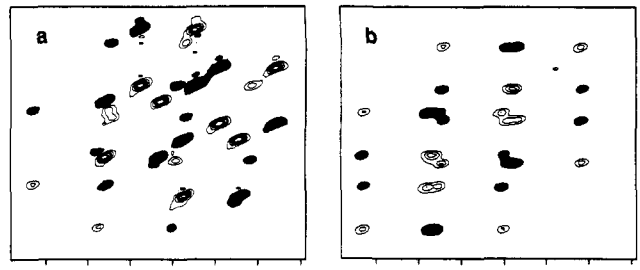

Figure 6. Multiplets obtained with (a) normal soft-COSY and (b) with SIS-(0,1)-COSY experiments performed on the A^{cis}–X^{cis} cross-peak in **1**. The multiplets were all obtained with a Bruker AM 400 spectrometer equipped with an Oxford Research Systems Selective Excitation Unit. The 270° pulses were all 35 ms in duration and the G^3 inversion pulses had a duration of 110 ms. The matrices consisted of 70 × 1K data points before and 256 × 1K data points after zero filling. A Lorentz–Gauss transformation was applied (LB = −0.5, GB = 0.15) before Fourier transformation. The spectral widths in the ω_1 and ω_2 domains were 35 and 250 Hz; only a section of 30 × 35 Hz is shown in the figures.

Phase Shifts Induced by Transient Bloch–Siegert Effects. Before implementing the SIS-(1,0)-COSY technique we should be aware of a practical problem associated with inserting selective RF pulses into the evolution time of an experiment. We have recently pointed out that although selective pulses will have no effect on the magnitude of the magnetization outside the "bandwidth" of the pulse, nevertheless they may induce substantial z-rotations over a frequency range many times wider.[40] These so-called transient Bloch–Siegert phase shifts are directly relevant to SIS-(p,q)-COSY experiments using t_1-PSFs with an inversion pulse on alternate scans ("on/off alternation", see above). In these circumstances the phase shifts will lead to imperfect suppression of unwanted coherences. To overcome this problem, we could implement phase cycling as in eq 5, in which case the transient phase shift would be the same for both scans.[40] This would however be at the sacrifice of frequency selectivity, as shown in Figure 2. Alternatively, we can simply calculate what the phase shift is and include a suitable correction to the RF phase of our pulses. When a PSF is applied at frequency Ω_{P1}, the induced phase shift at the center of the multiplet of spin I^{A1} is

$$\Delta\phi_{A1} = \langle\Delta\omega\rangle t_p \qquad (16)$$

where $\Delta\phi_{A1}$ is the phase shift experienced by the magnetization of spin I^{A1}, t_p is the overall length of the selective inversion pulse (e.g. of the G^3 cascade), and $\langle\Delta\omega\rangle$ is the average deviation of the magnitude of the tilted effective field experienced by spin I^{A1} from the offset with respect to Ω_{P1}, i.e. from the effective field that I^{A1} would experience in the t_p interval in the absence of an inversion pulse[40]

$$\langle\Delta\omega\rangle = \langle|\Omega_{A1}^{eff}| - (\Omega_{A1} - \Omega_{P1})\rangle \qquad (17)$$

where the average is taken over time-dependent frequencies with the instantaneous values of $\Omega_{A1}^{eff} = [(\Omega_{A1} - \Omega_{P1})^2 + \omega_1(t)^2]^{1/2}$. Assuming that the phase shift is constant over the width of the multiplet, we may then simply shift the phase of the pulse at the end of t_1 accordingly. Note that this pulse creates populations which have no phase memory. A standard Pascal program for Aspect, Sun, or VAX computers to calculate transient Bloch–Siegert phase shifts for some common pulse shapes is available on request. For some typical pulses, intended to invert passive spin multiplets that are 20–60 Hz wide, exemplary phase corrections are given in Table II.

Application and Discussion

We have applied the SIS-(0,1)-COSY sequence of Figure 4 to a 1:3 mixture of *cis*- and *trans*-2-phenylcyclopropanecarboxylic acid methyl ester (**1**) (R = $COOCD_3$, R′ = C_6H_5). The normal

(40) Emsley, L.; Bodenhausen, G. *Chem. Phys. Lett.* **1990**, *168*, 297.

(soft) COSY spectrum yields cross-peak multiplets (A^{cis}, X^{cis}) and

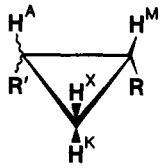

1

(A^{trans}, X^{trans}) that are severely overlapped for the two isomers (Figure 6a). The shifts of the passive coupling partners M^{cis} and M^{trans}, K^{cis} and K^{trans} are however all different. Applying the PSF to the passive spin K^{cis} results in the spectrum shown in Figure 6b. It can be seen that the multiplet arising from the dominant trans isomer has been removed by the filter, since for this case **P** matches $\mathbf{M}^{cis}$ but **P** does not match $\mathbf{M}^{trans}$. More specifically, for the cis isomer $P_{33} = M_{33}$, but for the trans isomer $P_{33} \neq M_{33}$. So in this case the only source of mismatch lies in the "color" (frequency) of the node P_{33} and not in any difference in connections between edges of the network. As expected the multiplet structure exhibits antiphase splittings due to J_{AX}, J_{AK}, and J_{XK}; in addition we can clearly see how two basic patterns are displaced with respect to each other by the couplings J_{AM} and J_{XM} to the remaining passive spin (see Figure 6). This highlights the fact that we have a matching condition corresponding to case ii above. This is easily distinguishable from the other conditions of matching and indicates that the fragment **M**, shown in Figure 3e, contains more couplings than are probed by the experiment **P**.

When it is necessary to apply m distinct filters in one experiment, we need $2^{(m+1)}$ scans for each t_1 increment, including the phase alternation of the first pulse that is required to suppress axial peaks. For $m = 2$, the cycle is given in Table III. If we must apply selective pulses at two different frequencies, this can be most effectively achieved by using cosine-modulated pulses.[41] We have verified this approach experimentally by implementing the SIS-(0,2)-COSY sequence of Figure 4 on the cyclopropane system and obtained the expected multiplet structure (not shown).

Figure 7 shows an example of the peak structure obtained in SIS-(1,0)-COSY applied to a valine NH–C^{α}H cross-peak in the cyclic undecapeptide cyclosporin A,[42] which corresponds to the system of Figure 3b where the C^{β}H proton is the passive spin, subjected to a PSF consisting of a 15 ms 180° Gaussian pulse on alternate scans. The C^{α}H and NH protons are active in t_1 and t_2, respectively. The offset between the chemical shifts of the passive C^{β}H and active C^{α}H protons is 900 Hz. The experiment was therefore compensated for a 6° transient Bloch–Siegert phase shift. To highlight the frequency selectivity of these filters, Figure 7c shows the effect of accidentally missetting the inversion pulse in the PSF to another multiplet belonging to a different system (at an offset of 100 Hz (=0.25 ppm) from the true passive C^{β}H proton). The suppression is seen to be excellent, the residual signals being a factor of 15 smaller than those of Figure 7b. This shows how the frequency bandwidth of the selective pulse (in this case a 180° Gaussian, see Figure 2) is sufficiently narrow to allow discrimination between fragments on the basis of the chemical shifts of passive spins, i.e. through mismatch of the diagonal elements of the matrices **P** and **M** (in this case $\dim(\mathbf{M}^{sub}) < \dim(\mathbf{P})$). Figure 7 also demonstrates that transient Bloch–Siegert phase shifts can be properly compensated for. We used a 180° Gaussian inversion pulse for this t_1-PSF in order to minimize the first-order frequency-dependent phase correction of the spectra in the ω_1 domain since a simple Gaussian is shorter than a G^3 Cascade to achieve the same bandwidth (although it sacrifices some selectivity in the "top-hat" sense, see Figure 2).

Figure 8 shows how the techniques can be used to assign the C^{α}H–C^{β}H-C^{γ}H connectivities in three of the amino acid residues of cyclosporin A. It can be seen that the cross-peaks originating

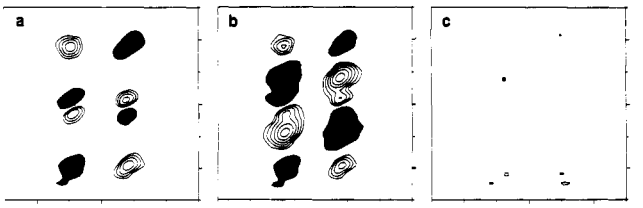

Figure 7. Multiplets obtained with (a) normal soft-COSY and (b) with new SIS-(1,0)-COSY experiments performed on the NH–C^{α}H cross-peak in the valine-5 residue of cyclosporin A (45 mg in 0.5 mL of $CDCl_3$). (c) The effect of missetting the transmitter frequency for the passive spin filter by ≈100 Hz (0.25 ppm) in the SIS-(1,0)-COSY experiment, highlighting the frequency selectivity of these filters. The first two pulses (35 ms 270° Gaussians) were applied to the C^{α}H at 4.66 ppm and the last pulse to the NH at 7.47 ppm. In (b) the PSF was applied to the C^{β}H at 2.14 ppm using a 15 ms Gaussian 180° pulse. The matrices consisted of 64 × 512 and 256 × 1K data points before and after zero filling, recorded with spectral widths in the ω_1 and ω_2 domains of 50 and 200 Hz (30 × 30 shown) with 4 scans per t_1 increment. The total time for each experiment was about 4.5 min.

from each of the leucine-6, leucine-9, and valine-11 residues can be effectively isolated solely on the basis of their differing topologies, providing a simple way of obtaining a definite assignment of these fragments. Note that the separation of these multiplets is not dependent on the active spins having different chemical shifts but on differences in the shifts of *passive* (i.e., $C^{\beta'}$H) spins and on differences in the topologies of the networks, i.e., a linear valine C^{α}H–C^{β}H–$C^{\gamma}H_3$ fragment will not pass a τ_m-PSF. In this example, intended as a demonstration, the separation does not yield novel information, but if the multiplets in Figure 8a had been accidentally superimposed, filtration would greatly facilitate their analysis. Indeed, the separation would also be possible if the multiplets were completely overlapped as in the case of Figure 6.

The multiplet patterns obtained by a given experiment highlight the extent of matching or mismatching between the fragment and the experiment, i.e. between the matrices **M** and **P**. Some examples are shown in the simulations of Figure 5. Note especially how the absence of triplet structures in SIS-(p,0)-COSY experiments highlights the fact that a fragment with a cyclic topology is probed by an experiment designed for a linear topology. In the experimental spectra of Figure 8 we immediately see that the actual fragments are all larger than the test topologies used to probe them, as evidenced by the passive C^{β}H–C^{γ}H couplings which give rise to small in-phase doublets with a vertical displacement in Figure 8, c and d, and the passive C^{β}H–$C^{\gamma}H_3$ splittings in Figure 8a.

Equivalent Spins. Normally, one distinguishes two types of equivalence. Chemical equivalence occurs when several spins have the same shift but not necessarily the same coupling constants, while magnetically equivalent spins are the same in all respects. Although we have not mentioned it so far, equivalence can of course be included in our schemes, and in fact makes little difference. Nodes containing equivalent passive spins are noted as, for example, $\Omega_{P_i}^{[n]}$ where n is the number of equivalent spins, and a network containing equivalent spins is shown in Figure 3f. Since our experiments are not dependent on the actual value of $J_{A_iP_j}$, we cannot distinguish a priori between chemical and magnetic equivalence, as there is no difference in the topology of the network, as we have defined it.

Diagonal Multiplets. Finally, we should briefly mention that SIS-(p,q)-COSY experiments can also be used to probe the structure of diagonal multiplets, in which case $I^{A1} = I^{A2}$ and all three of the Gaussian pulses shown in the sequences of Figure 1 or 4 should be applied at the same frequency. In this case the relevant fragment topologies are simplified since there is only one active node, thus all passive spins must by definition be coupled to the active spin in both t_1 and t_2. As a result it is possible to use SIS-(0,q)-COSY for any type of fragment, thereby providing a means of unravelling diagonal multiplets from crowded spectral regions in order to obtain, for example, reference intensities for two-dimensional exchange or NOESY spectra in a similar way

(41) Emsley, L.; Burghardt, I.; Bodenhausen, G. *J. Magn. Reson.* **1990**, *90*, 214.

(42) Loosli, H.-R.; Kessler, H.; Oschkinat, H.; Weber, H.-P.; Petcher, T. J.; Widmer, A. *Helv. Chim. Acta* **1985**, *68*, 682.

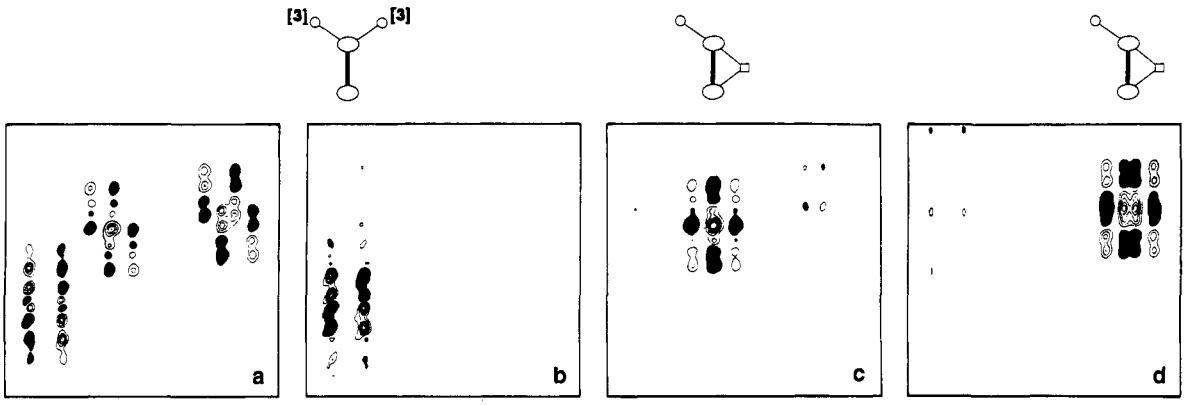

Figure 8. Topological filters applied to the cyclic undecapeptide cyclosporin A. (a) Normal soft-COSY of the region containing the $C^{\alpha}H$–$C^{\beta}H$ cross-peaks of valine-11, leucine-9, and leucine-6, centered at 2.15 ppm in ω_1 and 5.07 ppm in ω_2. (b) Same region for a SIS-(1,0)-COSY with the PSF applied at $\Omega_{C^{\gamma}H3}$ of valine-11. (c) Same region for a SIS-(0,1)-COSY with the PSF applied at $\Omega_{C^{\beta}H}$ of leucine-9 and (d) with the PSF applied at $\Omega_{C^{\beta}H}$ of leucine-6. Note how the cross-peaks are easily separable on the grounds of their topology. All 270° pulses were 15 ms in duration, the G^3 pulses used in τ_m-PSFs were 50 ms duration, while the 180° Gaussian pulses used in t_1-PSFs were 15 ms. The experiment in (b) is compensated for a 10° Bloch–Siegert phase shift. The spectral widths in ω_1 and ω_2 were 100 and 200 Hz, respectively; sections of 90 × 90 Hz are shown.

Table II. Exemplary Bloch–Siegert Phase Shifts[a]

		offset,[b] Hz							
pulse	Δω,[d] Hz	100	200	300	400	500	600	800	1000
100 ms G^3	30	49.6	25.1	16.8	12.6	10.1	8.4	6.3	5.1
50 ms G^3	60	95.0	49.7	33.4	25.1	20.1	16.8	12.6	10.1
35 ms G^1[c]	22	21.7	11.0	7.4	5.5	4.4	3.7	2.7	2.2
12.5 ms G^1[c]	60	54.3	29.8	20.3	15.3	12.3	10.2	7.2	6.2

[a] Calculated according to eq 7 of ref 40 and expressed in deg. For values intermediate to those given, linear interpolation should suffice, while for other pulse shapes or lengths a utility program is available on request. [b] $\Omega_{A1} - \Omega_{P1}$. [c] A simple Gaussian pulse with 1% truncation. [d] Bandwidth over which inversion is >90% for G^3 and >70% for G^1.

Table III. Pulse Combinations Necessary for SIS-(p,q)-COSY Sequences with $p + q = 2$

scan no.	ϕ_1	Ω_{P1}	Ω_{P2}	receiver
1	$+y$	inverted	inverted	add
2	$+y$	inverted	NOP[a]	sub
3	$+y$	NOP	inverted	sub
4	$+y$	NOP	NOP	add
5	$-y$	inverted	inverted	sub
6	$-y$	inverted	NOP	add
7	$-y$	NOP	inverted	add
8	$-y$	NOP	NOP	sub

[a] NOP = no operation.

to the recently developed MUSIC technique (multiplets unravelled by selective injection of coherence).[27] Indeed, experiments using PSFs to separate relaxation pathways involving different forms of longitudinal spin order have been extensively used by Di Bari et al.[43] Such experiments allow one to access a wealth of information about the behavior of the molecule under investigation.

(43) Di Bari, L.; Kowalewski, J.; Bodenhausen, G. *J. Chem. Phys.* **1990**, *93*, 7698.

Conclusions

We have shown how simple building blocks can be combined to give a new family of SIS-(p,q)-COSY experiments which are very powerful to distinguish fragments belonging to networks of coupled spins on the basis of their topology. The signal-to-noise per unit time is generally much higher than that for a normal nonselective COSY experiment, although it nevertheless decreases as the number of multiplet components increases (see Figure 5), except when a SIS-(p,0)-COSY type experiment is applied to a linear network in which case the signal-to-noise actually improves (barring accidental cancellations). The experiments can be used as an attractive and time-saving alternative to three and higher dimensional spectroscopy in order to unravel crowded spectra (as in Figure 6). The experiments are useful not only to discriminate between overlapping signals but also to confirm the assignment of spin systems.

Acknowledgment. We are grateful for many illuminating discussions with all the members of the Lausanne Spin Department, especially Peter Huber and Lorenzo Di Bari, and for helpful comments from the referees. This work was supported in part by the Swiss National Science foundation, by the Commission pour l'Encouragement de la Recherche Scientifique, and by Spectrospin AG, Fällanden, Switzerland.